1. Tanakorn INTHASUTH, 2. Natapon KAEWTHONG, 3. Robithoh ANNUR, 4. Kritsana SUREEYA

ORCID: 1. 0000-0002-3682-7080; 2. 0009-0005-8346-6619; 3. 0000-0002-0761-1192; 4. 0009-0008-2304-6681

OPEN ACCESS

DOI: 10.15199/48.2025.06.09

Enhancing battery life and energy efficiency in solar-powered IoT devices through cyclic sleep control system

Zwiększanie żywotności baterii i efektywności energetycznej w urządzeniach IoT zasilanych energią słoneczną poprzez system cyklicznego uśpienia

Abstract: *The unstable operation of Internet of Things (IoT) devices installed outdoors, which rely on solar energy, is often caused by insufficient power supply or battery degradation. This paper presents a cyclic sleep control system (CSCS) for an IoT-based air quality monitoring system utilizing Narrowband Internet of Things (NB-IoT) technology, deployed in Songkhla Municipality. The objective is to enhance sensor data availability (SDA) across monitored zones over a seven-day period. Experimental results showed that SDA was only 4.2% without CSCS. After implementing CSCS, SDA significantly improved in all zones—for example, Zone A increased from 66.7% to 87.5%, and Zone D achieved 100% availability. The CSCS effectively reduces energy consumption and supports continuous 24-hour operation. Importantly, the system was integrated without any hardware modifications, demonstrating the practicality of CSCS as a low-cost and non-invasive solution for improving IoT system reliability in solar-powered deployments.*

Streszczenie: *Niestabilna praca urządzeń Internetu Rzeczy (IoT) instalowanych na zewnątrz, zasilanych energią słoneczną, często wynika z niewystarczającego zasilania lub degradacji baterii. W niniejszym artykule przedstawiono system cyklicznego uśpienia (CSCS) dla systemu monitorowania jakości powietrza opartego na technologii Narrowband Internet of Things (NB-IoT), wdrożonego w gminie Songkhla. Celem jest zwiększenie dostępności danych z czujników (SDA) w monitorowanych strefach w ciągu siedmiodniowego okresu. Wyniki eksperymentalne wykazały, że SDA wynosiła jedynie 4,2% bez zastosowania CSCS. Po wdrożeniu CSCS, SDA znacznie poprawiła się we wszystkich strefach — na przykład w Strefie A wzrosła z 66,7% do 87,5%, a w Strefie D osiągnęła 100% dostępności. CSCS skutecznie redukuje zużycie energii i umożliwia ciągłą, 24-godzinną pracę. Co istotne, system został zintegrowany bez modyfikacji sprzętowych, co potwierdza praktyczność CSCS jako niskokosztowego i nieinwazyjnego rozwiązania poprawiającego niezawodność systemów IoT zasilanych energią słoneczną.*

Keywords: IoT, sleep-awake cycle, AQI sensor, smart city
Słowa kluczowe: IoT, cykl snu i czuwania, czujnik AQI, inteligentne miasto

Introduction

When Internet of Things (IoT) devices are deployed outdoors, a reliable communication channel with real-time interaction is essential, as these devices need to remain connected and accessible most of the time. Various studies have explored IoT applications in outdoor environments, addressing needs such as air quality monitoring, location tracking, and fire detection. For instance, low-power wide-area network (LPWAN)-based systems have been implemented with sensors measuring pollutants such as NO_2, SO_2, CO_2, CO, and PM2.5, along with environmental parameters like temperature and humidity, transmitting data to a gateway (GW) for visualization on platforms like ThingSpeak [1]. Similarly, IoT combined with machine learning has been utilized for predicting outdoor air quality [2], while global positioning system (GPS) and general packet radio service (GPRS)-based location tracking systems provide 10–20 meters accuracy, although they require battery recharging every 15 days [3]. Additionally, IoT-based fire detection systems using LPWAN and solar energy have proven effective in providing early warnings in off-grid areas, outperforming satellite-based solutions [4, 5].

Despite these advancements, energy management remains a critical challenge, particularly in outdoor applications where power sources are limited to solar energy and battery storage. Research on energy-efficient IoT systems has proposed various sleep-wake strategies to optimize battery life. For example, Age of Information (AoI) models have been applied to control sensor wake-up schedules based on data freshness requirements [6]. Other approaches utilize deep sleep modes with real-time clock (RTC) control to extend battery life [7], while scheduler-based mechanisms have been designed to reduce power consumption during network collisions or failures [8].

Between 2020 and 2021, Songkhla Municipality, in collaboration with Rajamangala University of Technology Srivijaya, launched a smart city initiative deploying solar-powered IoT-based air quality indicators (AQI) at four locations: Zones A, B, C, and D. These nodes, illustrated in Fig. 1 as part of the system architecture, were installed in public areas such as a university, schools, and a market, utilizing Narrowband IoT (NB-IoT) technology to transmit data to a cloud-based monitoring platform [9]–[11]. The actual hardware setup, shown in Fig. 2, included environmental sensors, solar panels, and NB-IoT modules installed on-site. The system was designed to provide real-time PM2.5 monitoring and public notifications through social media platforms such as LINE and Facebook [9]. While the system succeeded in raising public awareness, it occasionally experienced data transmission delays. However, performance evaluations indicated that the system maintained an average round-trip time (RTT) of 2–5 seconds, with automatic packet retransmissions compensating for temporary communication losses of up to 30 seconds [10]. Further analysis revealed that battery degradation significantly impacted data accuracy, particularly during early mornings and evenings when solar energy input was low [11].

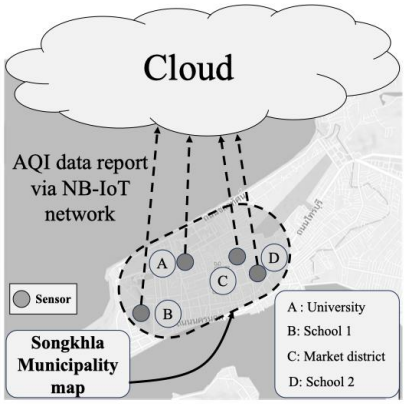

Fig. 1. Overview of IoT-based AQI device deployment locations.

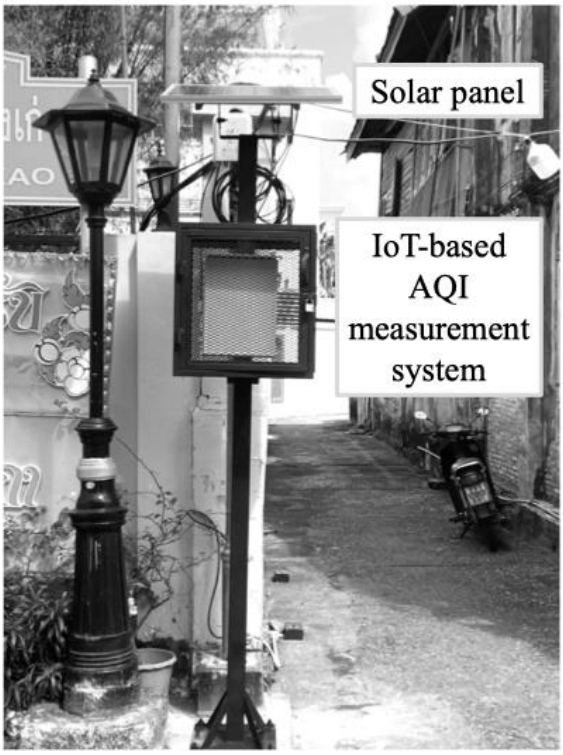

Fig. 2. Actual hardware setup of the deployed IoT-based AQI monitoring system.

Additionally, the AQI sensors required substantial power during warm-up periods of 1–2 minutes, making continuous operation challenging without effective energy management strategies. Prior studies have suggested that optimizing the sleep-wake cycle, similar to techniques employed in ZigBee [13] and NB-IoT systems [14], could help mitigate these challenges.

While several energy-saving techniques [15–17] have been proposed for general IoT systems, limited research has specifically addressed the implementation of a cyclic sleep control system (CSCS) for solar-powered NB-IoT-based air quality monitoring systems in real municipal environments. To address this gap, this paper proposes and evaluates a CSCS designed to improve both energy efficiency and data availability. The CSCS achieves this by reducing idle power consumption through periodic switching between active and sleep modes, making it particularly beneficial for sensors operating on aging batteries that might otherwise fail to function continuously.

This study makes three key contributions. First, it presents the design and integration of a low-cost CSCS that can be applied to existing NB-IoT-based air quality monitoring systems without requiring additional hardware modifications. Second, it provides real-world validation of the proposed CSCS in an operational municipal deployment covering four distinct monitoring zones. Third, it offers an empirical analysis demonstrating the system's ability to improve energy efficiency while maintaining data availability.

CSCS Implementation and Improvement

This section presents improvements to an existing outdoor IoT-based air quality monitoring system that previously experienced reliability issues due to aging batteries. Instead of replacing the hardware or discarding partially functional batteries, the research team implemented a low-cost CSCS to optimize energy usage. The CSCS allows sensor nodes to enter sleep mode during non-critical periods, reducing power consumption while maintaining data availability. This enhancement extends battery life and improves system efficiency without requiring modifications to the original circuit design.

1) Existing AQI detection system

The existing sensor device (Fig. 3) and GW (Fig. 4) form the core of the previously operational AQI detection system, which monitors environmental pollutants and reports real-time air quality. The system measures particulate matter, including PM2.5 and PM10.0, as well as gases such as O_3, CO_2, NO_2, SO_2, and NH_3. As described earlier, the sensors generate analog signals, which are converted to digital form and processed by a microcontroller to determine pollutant concentrations. The sensing system uses RS485 communication to interconnect multiple sensors with the GW. This communication employs universal asynchronous receiver and transmitter (UART) digital signal transmission over distances of 1–2 meters, providing reliable data transfer in electrically noisy environments and supporting the expansion of multiple sensors.

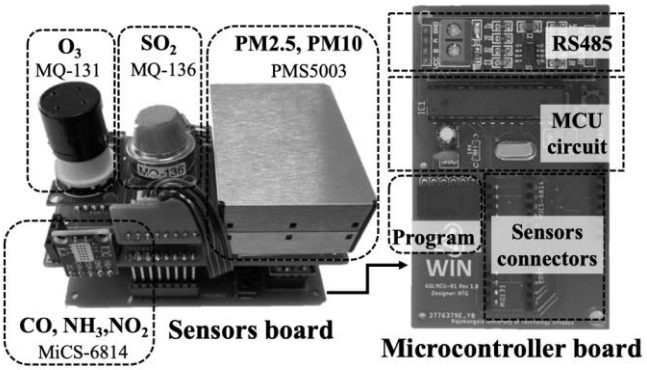

Fig. 3. AQI sensor based on RS485 communication

Fig. 4. GW module converting RS485 sensor data to NB-IoT for cloud transmission

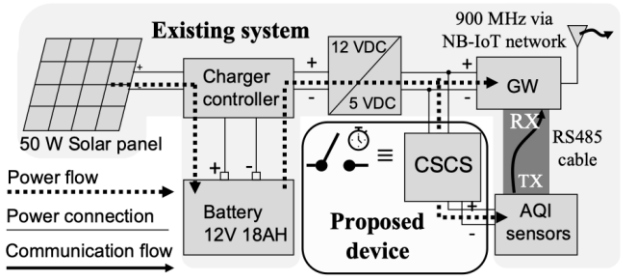

Fig. 5. Proposed diagram of CSCS implementation in an existing system

The MEGA Pro 2560 microcontroller in the system processes sensor data efficiently. The collected AQI data is transmitted to the cloud using an NB-IoT module, enabling low-energy, long-range data transfer. The GW utilizes the constrained application protocol (CoAP) to transfer real-time data to an IoT platform for monitoring and logging purposes. The system is powered by solar cells, supporting continuous operation in outdoor environments. It has been in operation for 1–2 years, but has experienced several issues related to energy storage degradation in aging batteries.

2) System improvement with CSCS

To address the energy limitations, a practical and immediate solution is to integrate a low-cost hardware component known as the CSCS, which reduces energy consumption by alternating the system between active and sleep states. As illustrated in Fig. 5, the proposed system comprises two main components: (1) the existing IoT-based AQI sensor unit, including a solar panel, charge controller, battery, and GW; and (2) an efficient CSCS designed to optimize power usage for sensors with high energy demands. Fig. 6 illustrates the CSCS hardware and its installation. The system significantly reduces power consumption during idle periods, thereby enhancing sustainability and prolonging the system's operational life. This technique is energy efficient, as it activates power only when necessary, minimizing waste and maximizing performance.

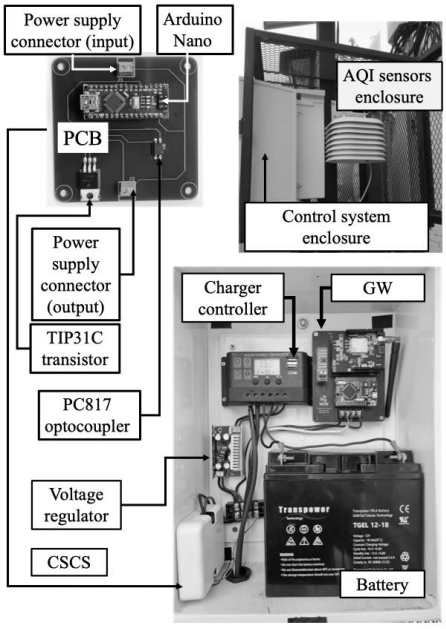

Fig. 6. Installation of CSCS hardware in an existing system

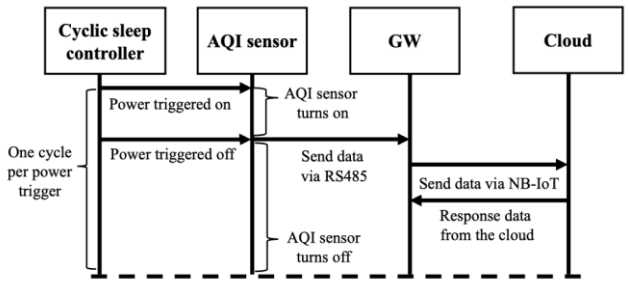

Fig. 7. Timing diagram of the IoT-based AQI monitoring system and the CSCS-based energy saving improvement

To better illustrate the application of the CSCS, the operational process is presented using an IoT timing diagram, as shown in Fig. 7. This sequence demonstrates how CSCS enhances energy management by systematically controlling power cycles. The controller periodically supplies power to the AQI sensor, activating it only during critical sensing intervals. Once activated, the AQI sensor begins collecting air quality data, which is then transmitted to the GW via RS485 communication. Subsequently, the GW forwards the data to the cloud using NB-IoT technology. After the cloud processes the data, a response is sent back to the GW. Following this, the AQI sensor powers down, entering a sleep state until the next cycle begins. This alternation between active and sleep states effectively reduces power consumption while maintaining reliable data communication. The use of CSCS enables the system to operate efficiently, particularly in scenarios with limited power availability.

Fig. 8(a) presents the energy profile of the existing system, highlighting the periods when the AQI sensor is active and when the NB-IoT module transmits data. It further reveals constant power consumption by the GW and NB-IoT module while in standby mode, underscoring the need for power optimization.

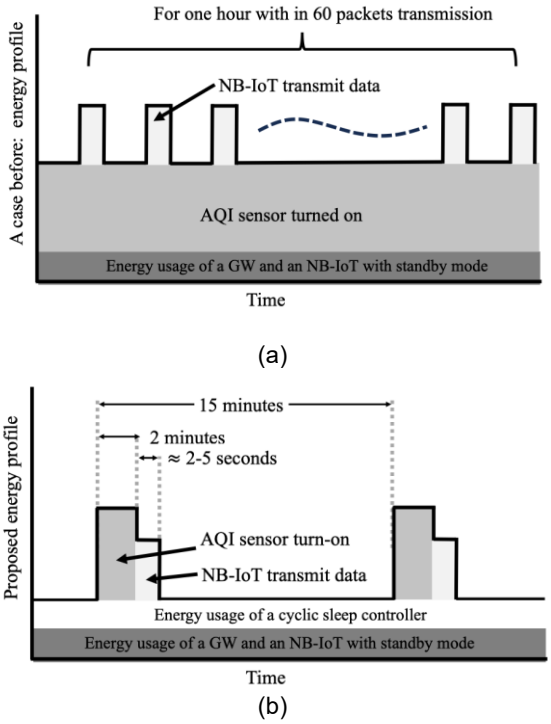

Fig. 8. Comparison of energy profiles: (a) before applying CSCS and (b) after applying CSCS

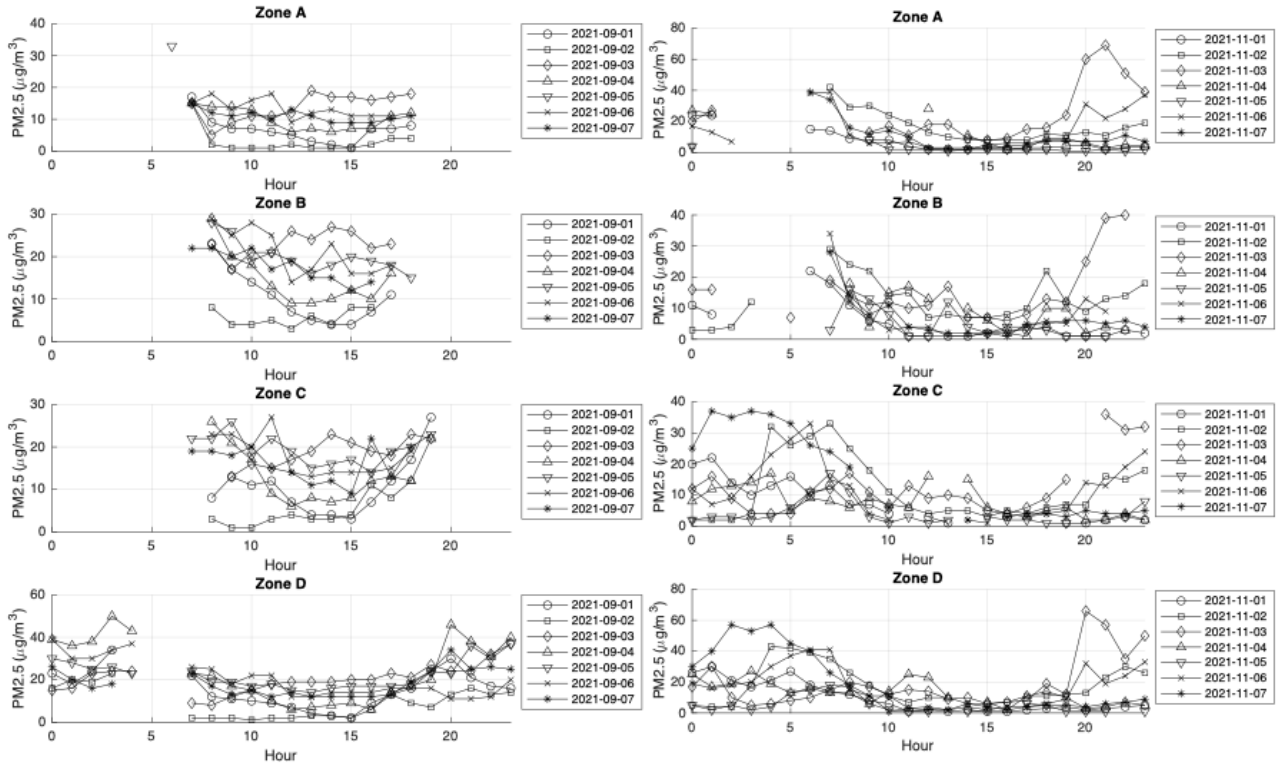

Fig. 9. PM2.5 time-series data across Zones A, B, C, and D over 24 hours for 7 consecutive days: (a) without CSCS implementation and (b) with CSCS implementation

Following the implementation of CSCS, as shown in Fig. 8(b), the AQI sensor operates for approximately 2 minutes, followed by NB-IoT data transmission. For the majority of the time, the controller significantly reduces energy consumption, enhancing system efficiency. The 15-minute operating cycle represents an effective balance between energy usage, data quality, sensor lifespan, and network load, making it a practical solution for long-term IoT deployment. During each cycle, the sensor remains active for only 2 minutes, while the remaining 13 minutes are spent in sleep mode, conserving power and extending the system's operational lifespan. The Arduino Nano-based controller manages the transitions between active and sleep states using a PC817 optocoupler and a TIP31C transistor. This solution requires only minor modifications to the electronic circuit of the previously installed system, ensuring that implementation costs remain minimal.

Experimental results and discussion

In this section, a comparative analysis is presented on PM2.5 time-series data continuity, sensor data availability, and the improvement in system performance before and after the implementation of the CSCS. The experimental results are also discussed in detail.

1) Time-series data without CSCS implementation

In Fig. 9(a), an experiment was conducted to collect PM2.5 data over a 7-day period from four areas—Zones A, B, C, and D—to compare system performance before and after implementing CSCS for energy saving. After collecting the data via the cloud-based system, it was observed that prior to CSCS implementation, the IoT system could not operate continuously for 24 hours due to battery degradation. Specifically, Zones A, B, and C exhibited similar patterns of data loss during nighttime periods. Zone D demonstrated better data continuity than the other zones, as the battery had been replaced earlier in the experiment. However, even in Zone D, continuous 24-hour operation was not achieved, likely due to limitations in the device's original design, which may not have fully considered real-world operating conditions. Additionally, PM2.5 data in Zones A, B, and C were completely missing during nighttime, indicating that the system was unable to store sufficient energy from the solar power source. Nevertheless, when comparing the data during the same time periods, the PM2.5 trends—including increases and decreases—were similar across all four zones, despite minor environmental differences, as all zones were located within the same municipal area.

2) Time-series data with CSCS implementation

In Fig. 9(b), after integrating the CSCS into the existing system, it was found that energy savings were achieved. However, the extent of performance improvement was initially unclear. In this experiment, the system was configured to operate in a 15-minute cycle, with 2 minutes of activity followed by 13 minutes of sleep. The results showed that the performance and continuity of data reporting were significantly improved, with the system successfully operating continuously throughout the day. Although in some areas, such as Zones A and B, the system still underperformed compared to Zones C and D, the daily PM2.5 measurement trends remained consistent across all zones, indicating that the data accuracy was preserved. These results highlight the benefits of extending battery life and reducing the frequency of battery replacements, which also contributes to minimizing environmental impact by reducing battery waste disposal. Therefore, the use of CSCS presents a practical and effective solution for extending system lifespan and enhancing operational reliability.

3) Sensor data availability comparison

The performance of the data monitoring system is evaluated by analyzing time-series data collected before

and after the implementation of the CSCS. As discussed in the previous subsection, the graphs illustrated that, during continuous operation without CSCS, data gaps occurred due to battery degradation, resulting in inconsistent monitoring. The integration of CSCS successfully enabled the sensor to operate on a controlled cycle, meeting monitoring requirements during critical periods while avoiding significant operational interruptions. This approach significantly improved data coherence, maximizing the utilization of residual battery power and enhancing the overall reliability of the system. To quantitatively assess this improvement, the sensor data availability (SDA) factor is calculated using Equation (1):

$$SDA = \frac{Uptime}{Uptime + Downtime} \tag{1}$$

where *Uptime* refers to the total duration during which the system is functioning correctly, and *Downtime* refers to the duration when the system is not operational. Both Uptime and Downtime are measured within a 24-hour monitoring period. This equation provides a quantitative measure of system availability, independent of subjective definitions of thresholds or failure classifications. As such, it serves as an objective metric for comparing the effectiveness of the CSCS before and after implementation.

Zone	Date/Hour	0	1	2	3	4	5	6	7	8	9	10	11	12	13	14	15	16	17	18	19	20	21	22	23	Data Availability (%)
A	2021-09-01									9	7	7	6	5	3	2	1	7	7	8						45.8
	2021-09-02									2	1	1	1	2	1	1	1	2	4	4						45.8
	2021-09-03									5	9	11	11	12	19	17	17	16	17	18						45.8
	2021-09-04								17	14	13	9	6	7	6	7	7	11	12							50
	2021-09-05							33																		4.2
	2021-09-06								15	18	13	16	18	9	12	13	11	11	11							45.8
	2021-09-07								15	12	11	12	10	13	11	9	9	9	10	11						50
B	2021-09-01									23	17	14	11	7	5	4	4	7	11							41.7
	2021-09-02									8	4	4	5	3	6	4	8	8								37.5
	2021-09-03									23	17	21	21	26	24	27	26	22	23							41.7
	2021-09-04									29	20	18	13	9	9	10	12	10	16							41.7
	2021-09-05									28	26	19	21	19	16	18	20	19	18	15						45.8
	2021-09-06									29	25	28	25	14	17	23	16	16	18							41.7
	2021-09-07								22	22	20	22	17	19	15	15	12	14								41.7
C	2021-09-01									8	13	11	12	7	4	4	3	7	12	17	27					50
	2021-09-02									3	1	1	3	4	3	3	4	11	8	12						45.8
	2021-09-03										13	16	15	17	19	23	21	19	18	23	22					45.8
	2021-09-04									26	21	17	9	6	8	7	8	12	13	12	22					50
	2021-09-05								22	22	26	18	22	19	15	16	17	14	19	20	23					54.2
	2021-09-06									23	23	20	27	14	13	14	14	14	15	19						45.8
	2021-09-07								19	19	18	20	15	14	11	12	9	22	13	20						50
D	2021-09-01	23	18	24	34				22	12	11	10	9	7	4	3	2	9	13	16	24	30	21	17	16	87.5
	2021-09-02	16	20	19	23				2	2	2	1	2	2	3	3	2	6	13	9	7	13	16	13	14	87.5
	2021-09-03	15	16	23	24	24			9	8	12	15	18	19	19	19	20	20	23	21	27	24	24	32	37	91.7
	2021-09-04	39	36	38	50	43			23	22	17	15	10	6	7	8	9	6	14	17	20	46	38	31	40	91.7
	2021-09-05	30	28	25	26	23			24	19	19	17	18	15	14	16	17	17	17	18	24	23	36	30	37	91.7
	2021-09-06	39	30	30	34	37			26	25	18	22	22	12	12	14	14	14	16	16	16	11	11	12	20	91.7
	2021-09-07	26	20	16	18				23	17	13	15	12	14	12	12	12	12	13	19	24	34	25	26	25	87.5

(a)

Zone	Date/Hour	0	1	2	3	4	5	6	7	8	9	10	11	12	13	14	15	16	17	18	19	20	21	22	23	Data Availability (%)
A	2021-11-01	24	24					15	14	9	8	8	4	2	2	2	3	2	3	3	4	5	2	3	4	83.3
	2021-11-02	4							42	29	30	24	19	13	10	8	8	8	8	12	11	13	11	16	19	75
	2021-11-03	20	27								13	17	11	18	18	9	8	9	15	16	24	60	69	51	39	70.8
	2021-11-04	27	25											28		11	6	2	3	9	9	6	3	5	4	54.2
	2021-11-05	4									8	2	2	2	1	2	2	2	2	2	1	1	2	1	2	66.7
	2021-11-06	17	13	7				38	39	11	6	6	7	3	2	2	5	6	6	8	8	31	22	28	37	87.5
	2021-11-07							39	34	16	12	14	10	3	3	3	3	4	5	7	7	7	7	11	7	75
B	2021-11-01	11	8					22	18	11	6	5	1	1	1	1	2	3	3	4	1	1	1	3	2	83.3
	2021-11-02	3	3	4	12				29	24	22	14	15	7	8	7	7	8	10	22	12	9	13	14	18	87.5
	2021-11-03	16	16				7		19	14	11	12	10	11	17	7	7	6	8	13	12	25	39	40		79.2
	2021-11-04									18	4	15	17	13		10	6	2	1	10	10	2	4	3		58.3
	2021-11-05								3	16	13	8	1	1	12	4	2	4	4	3	1	1	1			62.5
	2021-11-06								34	12	7	3	4	4	1	1	2	2	4	6	5	13	9			62.5
	2021-11-07								28	14	8	11	4	3	2	2	2	1	5	5	6	6	5	6	4	70.8
C	2021-11-01	20	22	14	10	13	16	10	13	7	7	4		3	1			3			1	1	2	3	2	79.2
	2021-11-02	2	2	2	4	32	26	29	33	25	18	11	6	4	5	5	3	5	4	6	7	7	16	15	18	100
	2021-11-03	12	16	9	4	4	4	11	12	17	11	6	13	9	10	9	5	4	6	9	15		36	31	32	95.8
	2021-11-04	8	12	13	14	17	5	9	8	6	9	7	6	16		15	6	4	3	5	6	2	2	4	2	95.8
	2021-11-05	2	3	3	2	3	6	11	17	11	3	1	3	1	2		3	2	2	1	1			3	8	87.5
	2021-11-06	12	7	9	16	23	28	33	15	13	4	2				2	1		3	4	5	14	13	19	24	83.3
	2021-11-07	25	37	35	37	36	33	26	24	19		6				2		3	4	4	3	5	4	4	5	79.2
D	2021-11-01	26	30	21	17	21	27	18	14	12	8	6	1	2	1	2	1	1	2	3	4	2	3	4	5	100
	2021-11-02	5	4	4	18	43	42	39	35	26	18	11	7	10	10	6	6	7	11	11	12	13	23	30	26	100
	2021-11-03	17	30	10	5	6	8	10	15	20	17	12	15	14	9	10	6	7	8	19	12	66	57	35	50	100
	2021-11-04	25	17	19	27	19	13	16	13	13	6	14	25	23	10		7	2	11	14	10	3	4	7	5	95.8
	2021-11-05	5	2	5	2	4	13	15	18	17	6	2	1	1		1	2		6	5	1	1	1		1	87.5
	2021-11-06	19	16	18	20	30	37	41	41	15	11	1	3	4	2	4	2	4	4	6	9	32	19	24	33	100
	2021-11-07	30	40	57	53	57	45	40	26	18	11	11	3	2	2	6	4	2	4	5	5	4	6	7	9	100

(b)

Fig. 10. Average hourly PM2.5 data over 24 hours and SDA: (a) before implementing CSCS and (b) after implementing CSCS

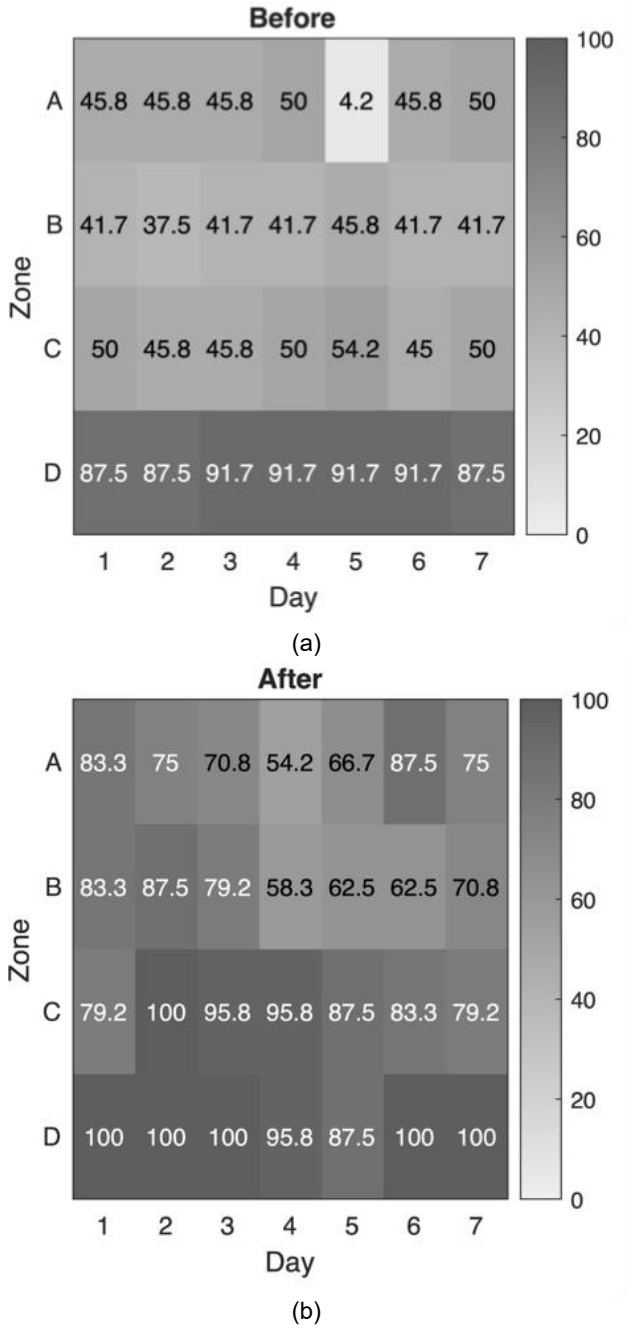

Fig. 11. Comparison of average daily PM2.5 data over a 7-day period and SDA: (a) before CSCS implementation and (b) after CSCS implementation

Figs. 10(a) and 10(b) illustrate the hourly patterns of data availability, where light-colored areas represent data collected during downtime, and dark-colored areas represent data collected during uptime across the four zones—Zones A, B, C, and D—before and after the implementation of the CSCS. These figures reflect the efficiency of data collection and the reliability of the system across the network. Prior to applying the CSCS, SDA remained relatively low, ranging from 37.5% to 54.2%, with significant downtime periods distributed throughout the day.

The readings for Zones A, B, and C were somewhat irregular and unpredictable, demonstrating inefficiencies in both sensor operation and energy usage. Although Zone D exhibited slightly higher availability, some irregularities remained, likely due to battery limitations. Extended sensor operation accelerated battery degradation, leading to erratic monitoring and persistent data gaps, particularly between 5 and 15 hours.

However, after the CSCS was implemented, SDA increased significantly, reaching 62.5% to nearly 100% across all zones. Zones C and D achieved 90% availability, demonstrating the controller's effectiveness in managing sensor operation and optimizing power consumption. Although Zones A and B still exhibited minor fluctuations, they showed notable improvements in both data availability and operational stability. The CSCS successfully activated the sensors during critical monitoring periods, maintaining an optimal power on/off cycle to conserve energy and extend battery life. This improvement underscores the controller's role in addressing operational irregularities, leading to enhanced monitoring uniformity and greater data reliability, particularly during critical pollution periods.

Figs. 11(a) and 11(b) present the average SDA before and after the implementation of CSCS, highlighting varying performance across the monitored zones. The summarized results are shown in Table 1. Overall, the results show that before CSCS, data availability was generally low and inconsistent, particularly in Zones A, B, and C. After CSCS implementation, all zones exhibited significant improvements, with Zones C and D achieving near-continuous data availability. These findings confirm the effectiveness of CSCS in enhancing system reliability and energy management.

The findings highlight the positive impact of the cyclic sleep method on data availability in the evaluated IoT-based monitoring system. By implementing this method, significant improvements were observed across all zones, resulting in higher data availability during the post-cyclic sleep phase. The method effectively reduced energy consumption during idle periods, extending the operational lifespan of the IoT devices while enhancing their data collection and transmission capabilities. The average data availability for each zone before and after applying the cyclic sleep method is summarized in Fig. 12.

Table 1: Summary of SDA before and after CSCS implementation

Zone	SDA before CSCS (%)	SDA after CSCS (%)
A	4.2 – 50.0	66.7 – 87.5
B	37.5 – 45.8	58.3 – 87.5
C	45.8 – 54.2	79.2 – 100.0
D	87.5 – 91.7	87.5 – 100.0

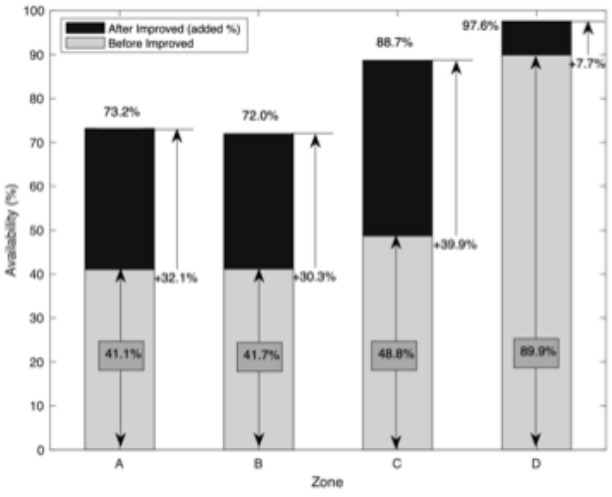

Fig. 12. Comparison of SDA before and after improvement across zones

These results indicate a significant improvement in SDA across all zones after implementing the cyclic sleep method. Zone C showed the highest increase in average availability, going from 48.8% to 88.7%. Zone D had the highest initial average SDA but still experienced a notable improvement. The increased SDA suggests that the cyclic sleep method effectively optimized energy consumption and enhanced the performance of the IoT system in terms of data collection and transmission.

Conclusion

This paper proposes and evaluates a CSCS to enhance the energy efficiency and data availability of solar-powered IoT-based air quality monitoring systems. The implementation of CSCS significantly reduces idle power consumption by enabling periodic switching between active and sleep modes, which is especially beneficial for aging battery-powered sensors that would otherwise fail to operate continuously. Field test results from four monitoring zones demonstrate substantial improvements in SDA, achieving consistent 24-hour data transmission while extending battery life without requiring any hardware modifications. The findings confirm that CSCS is a practical, low-cost, and scalable solution suitable for outdoor IoT deployments operating under limited power supply conditions. Additionally, the approach has been shown to be compatible with existing NB-IoT-based systems. In future work, we aim to expand the performance evaluation by considering additional factors and metrics, such as latency, packet delivery ratio (PDR), communication reliability, energy consumption modeling, and system scalability. We also plan to integrate artificial intelligence (AI)-based diagnostics to enable automated anomaly detection and improve real-time decision-making for enhanced system resilience and reliability.

***Authors**: Asst. Prof. Tanakorn Inthasuth, Rajamangala University of Technology Srivijaya, Thailand; Asst. Prof. Dr. Natapon Kaewthong, Rajamangala University of Technology Srivijaya, Thailand; Dr. Robithoh Annur, Bandung Institute of Technology, Indonesia; Kritsana Sureeya, Thai-Nichi Institute of Technology, Thailand, Email: kritsana.sur@tni.ac.th (corresponding author).*

REFERENCES

[1] Jabbar W.A., Subramaniam T., Ong A.E., Shu'Ib M.I., Wu W., De Oliveira M.A., LoRaWAN-based IoT system implementation for long-range outdoor air quality monitoring, *Internet of Things*, 19 (2022), 100540.
[2] Moursi A.S., El-Fishawy N., Djahel S., Shouman M.A., An IoT enabled system for enhanced air quality monitoring and prediction on the edge, *Complex & Intelligent Systems*, 7 (2021), No. 6, 2923–2947.
[3] Velasquez N., Medina C., Castro D., Acosta J.C., Mendez D., Design and development of an IoT system prototype for outdoor tracking, *Proc. Int. Conf. Future Networks and Distributed Systems*, (2017), 1–6.
[4] Roque G., Padilla V.S., LPWAN based IoT surveillance system for outdoor fire detection, *IEEE Access*, 8 (2020), 114900–114909.
[5] Mohamad M.H., Rahim N., Baharudin E., Yunus M.M., Performance analysis of air monitoring system using 433 MHz LoRa module, *Przegląd Elektrotechniczny*, 100 (2024), No. 3, 223–227.
[6] Wang J., Cao X., Yin B., Cheng Y., Sleep–wake sensor scheduling for minimizing AoI-penalty in Industrial Internet of Things, *IEEE Internet of Things J.*, 9 (2021), No. 9, 6404–6417.
[7] García-Orellana C.J., Macías-Macías M., González-Velasco H.M., García-Manso A., Gallardo-Caballero R., Low-power and low-cost environmental IoT electronic nose using initial action period measurements, *Sensors*, 19 (2019), No. 14, 3183.
[8] Al-Janabi T.A., Al-Raweshidy H.S., An energy efficient hybrid MAC protocol with dynamic sleep-based scheduling for high density IoT networks, *IEEE Internet of Things J.*, 6 (2019), No. 2, 2273–2287.
[9] Kaewthong N., Inthasuth T., Jantongpoon J., Kwanthong N., Kanplumjit T., Self-management perception of people's network in Songkhla municipality towards air pollution, *Proc. 19th Nat. Environ. Conf.*, (2022), 50–56. (in Thai)
[10] Inthasuth T., Uarchoojitt P., Boonsong W., Kaewthong N., Time-based performance analysis of Narrowband Internet of Things (NB-IoT) for particulate matter monitoring system, *Proc. 2023 Int. Conf. Electronics, Information, and Communication (ICEIC)*, Singapore, (2023), 1–4.
[11] Chatasa T., Charoensawat P., Nakkliang N., Inthasuth T., Kaewthong N., Boonsong W., Tracking data faults in an IoT-based PM2.5 monitoring system using time series data: A case study in Songkhla Municipality, Thailand, *Proc. 2024 Int. Tech. Conf. Circuits/Systems, Computers, and Communications (ITC-CSCC)*, Okinawa, Japan, (2024), 1–4.
[12] Avancini D.B., Rodrigues J.J.P.C., Martins S.G.B., Rabêlo R.A.L., Al-Muhtadi J., Solic P., Energy meters evolution in smart grids: A review, *J. Cleaner Production*, 217 (2019), 702–715.
[13] Piyare R., Lee S.R., Performance analysis of XBee ZB module based wireless sensor networks, *Int. J. Scientific & Engineering Research*, 4 (2013), No. 4, 1615–1621.
[14] Alobaidy H.A., Singh M.J., Nordin R., Abdullah N.F., Wei C.G., Soon M.L.S., Real-world evaluation of power consumption and performance of NB-IoT in Malaysia, *IEEE Internet of Things J.*, 9 (2021), No. 13, 11614–11632.
[15] Bedewy A.M., Sun Y., Singh R., Shroff N.B., Low-Power Status Updates via Sleep-Wake Scheduling, *IEEE/ACM Trans. Networking*, 29 (2021), No. 5, 2129–2141.
[16] Jaworski D.J., Park A., Park E.J., Internet of Things for Sleep Monitoring, *IEEE Instrum. Meas. Mag.*, 24 (2021), No. 2, 30–36.
[17] Ye D., Zhang M., A Self-Adaptive Sleep/Wake-Up Scheduling Approach for Wireless Sensor Networks, *IEEE Trans. Cybernetics*, 48 (2018), No. 3, 979–992.